Studies in Fungi

ARTICLE

Open Access

https://doi.org/10.48130/sif-0025-0015
Studies in Fungi **2025**, 10: e015

Antifungal metabolite profiling and inhibition assessment of *Trichoderma*-derived compounds during initial spore germination stage against postharvest pathogens

Kamran Rahnama[1*], Nima Akbari Oghaz[1*], Nooshin Derakhshan[1] and Ruvishika Shehali Jayawardena[2,3]

[1] *Department of Plant Protection, Faculty of Plant Production, Gorgan University of Agricultural Sciences and Natural Resources, Gorgan, Golestan, 4918943464, Iran*
[2] *Center of Excellence in Fungal Research, Mae Fah Luang University, Chiang Rai, 57100, Thailand*
[3] *School of Science, Mae Fah Luang University, Chiang Rai, 57100, Thailand*
* Corresponding authors, E-mail: rahnama@gau.ac.ir; nimaakbarioghaz@gmail.com

Abstract

The objective of this study was to identify antifungal secondary metabolites produced during the early spore germination stage of *Trichoderma harzianum*, *T. virens*, and *T. atroviride* and evaluate their inhibitory effects on spore germination for 18 postharvest fungal species including *Alternaria*, *Aspergillus*, *Botrytis cinerea*, *Cladosporium*, *Fusarium*, and *Penicillium* on PDA medium supplemented with 200 µg/mL of secondary metabolites derived from each *Trichoderma* species. Secondary metabolites were extracted with ethyl acetate, diluted in n-hexane, and identified by Gas Chromatography-Mass Spectrometry (GC-MS) using a non-polar column and NIST23 library matching (≥ 85%). In comparation with control ($p \leq 0.05$), *T. atroviride* showed the highest inhibition of spore germination in *A. alternata* (39.93%), and *A. tenuissima* (37.97%). *T. harzianum* was most effective against *F. oxysporum* (40.84%); and *T. virens* inhibited *F. oxysporum* (37.02%), *A. alternata* (35.05%), *A. tenuissima* (37.05%), and *A. arborescens* (35.06%). Among 39 identified metabolites, 30.76%, 12.82%, and 15.38% originated from *T. atroviride*, *T. virens,* and *T. harzianum*, respectively. Furthermore, 23.07% were common to all three species. Additionally, 12.82% of the compounds were shared between *T. virens* and *T. harzianum*, while only 5.12% were shared between *T. atroviride* and *T. virens*. Several antifungal metabolites, including lauric acid, palmitic acid methyl ester, undecanoic acid, decanoic acid, itaconic acid, and hexadecanoic acid methyl ester, were identified during the initial spore germination stage of *Trichoderma* spp. The antifungal metabolites identified likely contribute to the ecological competitiveness of *Trichoderma* in the natural environment and underscore their potential in suppressing plant pathogens in agriculture.

Citation: Rahnama K, Oghaz NA, Derakhshan N, Jayawardena RS. 2025. Antifungal metabolite profiling and inhibition assessment of *Trichoderma*-derived compounds during initial spore germination stage against postharvest pathogens. *Studies in Fungi* 10: e015 https://doi.org/10.48130/sif-0025-0015

Introduction

According to the United Nations Food and Agriculture organization (FAO), postharvest losses of agricultural commodities account for approximately 14% of total production[1]. Pathogenic fungi are a major cause of these losses, affecting the quality, nutritional value, and marketability of stored produce. *Aspergillus* species, notably *A. flavus* and *A. niger*, are significant due to their production of aflatoxins, classified as Group 1 human carcinogens by the International Agency For Research on Cancer (IARC)[2]. *Penicillium* molds infect fruits, vegetables, grains, and stored products such as apples and citrus fruits, reducing marketability and posing health risks through mycotoxins like ochratoxin A[3]. *Botrytis cinerea* is a versatile pathogen causing grey mold across multiple crops, including grapes and strawberries[4]. Certain *Fusarium* species produce harmful mycotoxins, such as deoxynivalenol and fumonisins affecting cereals like wheat and maize[5]. *Alternaria* species, like *A. alternata*, induce spoilage and may contaminate crops such as tomatoes and carrots with alternariol[6]. *Cladosporium* species contribute to crop decay and mycotoxin contamination, leading to further storage losses in cereals and fruits[7]. The use of chemical fungicides, such as Thiophanate-methyl, Prochloraz, Propiconazole, and others, is one of the most effective strategies for controlling postharvest plant pathogenic fungi in storage[8]. However, many of these fungicides raise health concerns. For example, Thiophanate-methyl is classified by the United States Environmental Protection Agency (US EPA) as a probable human carcinogen (Group C), while Prochloraz and Propiconazole are considered suspected endocrine disruptors and have shown carcinogenic potential in animal studies[9]. Prolonged exposure can cause skin, eye, and respiratory irritation, as well as affect the liver, blood, thyroid, endocrine function, reproductive health, and development. Overuse has also led to resistance in fungal pathogens[10].

Biological control offers an alternative, minimizing risks to human health and the environment[11,12]. *Trichoderma* spp. are well-known biocontrol agents in plant pathology[13,14], engaging in competitive interactions with pathogenic fungi for resources, thus inhibiting their growth[15]. These fungi can directly attack pathogens by entwining around their hyphae and producing lytic enzymes, such as chitinases, glucanases, and proteases, as well as antifungal metabolites[16]. Key antifungal compounds produced by *Trichoderma* include harzianic acid, trichodermin, gliotoxin, and others, which have demonstrated significant antifungal activity against various postharvest pathogens[17,18]. All studies have focused on competition and secondary metabolite production during the mature stages of *Trichoderma* growth. However, no research has explored the interactions during the early stages. Focusing on the spore germination stage may reveal unique metabolite profiles that are absent or undetectable during later stages of growth. This study aimed to identify secondary metabolites produced by *T. harzianum*, *T. virens*, and *T. atroviride* during their spore germination stage using Gas Chromatography-Mass Spectrometry (GC-MS), and to examine their effects on the germination of 18 postharvest pathogenic

fungi, including *Alternaria* spp., *Aspergillus* spp., *B. cinerea*, *Cladosporium* spp., *Fusarium* spp., and *Penicillium* spp. The spore germination stage is a critical phase in fungal life cycles, representing a window for rapid establishment and early competition, which is essential for effective biocontrol.

Materials and methods

Preparation and spore characterizations

To prepare standardized spore suspensions and characterize germination behavior, three species of the genus *Trichoderma* (*T. atroviride*, *T. harzianum*, *T. virens*) and 18 post-harvest plant pathogenic fungi were obtained from Gorgan University of Agricultural Sciences and Natural Resources, Iran (Table 1). The propagation of fungi was carried out on autoclaved potato dextrose agar (PDA) medium (Merck 110130). A mycelial disc (5 mm) from the stock culture was aseptically transferred onto PDA plates (pH 7.0). The plates were then incubated (Memmert IN110plus) at 25 ± 2 °C for three days, with a relative humidity of 60%. All culture and germination experiments were performed in triplicate to ensure reproducibility. The spore suspensions were prepared by scraping spores from actively growing cultures with a sterile loop into sterile distilled water. The suspensions were filtered through sterile 200-mesh gauze to remove mycelial fragments. The suspension was transferred into sterile 15 mL tubes and subjected to centrifugation at 5,000 rpm for 20 min. Following centrifugation, the supernatant was carefully removed using a sampler, and the resultant pellet, which contained the spores, was resuspended in sterile potato dextrose broth (PDB) medium (Himedia GM403) by transferring it to new tubes. The final spore concentration was adjusted to 1×10^5 spore/mL, using a hemocytometer. For each fungal species, 100 µL of spore suspension was placed on a sterile glass slide within a petri dish, covered with a sterile coverslip, and incubated at 25 ± 2 °C in continuous darkness. Spore germination tests were conducted in triplicate, and appropriate negative controls (slides without spores and without medium) were included to monitor background effects. Observations of spore germination and size (average of 100 spores) were made at 40× magnification using an Olympus CH20i light microscope, with spore size and germination recorded every 30 min.

Extraction of secondary metabolites

According to Siddiquee et al.[19], with slight modifications, each *Trichoderma* sp. was inoculated into a 250 mL Erlenmeyer flask containing 100 mL of sterile PDB medium using 10 mL of spore suspension (10^5 spores/mL). Three biological replicates (flasks) were prepared per species. The flasks were incubated at 26 ± 2 °C on an orbital shaking incubator (Benchmark B00BUA672E) with an agitation speed of 4 m/s² for 12 h, a duration selected to capture the early spore germination stage, before activating mycelial growth.

Table 1. Spore characteristics of fungal isolates.

Specific name	*GAU No.	**NCBI No.	Germination percentage after 12 h	Spore shape	Spore size (µm)		***Final germination length (µm)	End of germination time (h)	Germination speed (µm/h)
					Length	width			
Trichoderma atroviride	6022	MG807425.1	98.6 ± 0.40 ab	Ellipsoidal	3.979 ± 0.059 hijk	4.125 ± 0.057 d	5.968575	8.761 ± 0.092 e	0.681
T. harzianum	Ah90	KC576649.1	99.2 ± 0.37 ab	Oval	3.177 ± 0.057 ijk	3.152 ± 0.060 e	4.764825	8.884 ± 0.071 e	0.536
T. virens	6011	KP671477.1	99.4 ± 0.40 a	Oval	2.626 ± 0.029 k	2.595 ± 0.029 h	3.938745	11.800 ± 0.109 c	0.334
Penicillium implicatum	MK-RSB19	OP411018.1	99.0 ± 0.01 ab	Oval	2.852 ± 0.043 jk	2.905 ± 0.039 f	4.277535	14.780 ± 0.108 b	0.289
P. italicum	MK-RSB20	OP411019.1	99.0 ± 0.45 ab	Spherical	4.059 ± 0.055 hijk	4.149 ± 0.059 d	6.088485	14.823 ± 0.100 b	0.411
P. expansum	MK-RSB18	OP411020.1	98.6 ± 0.40 ab	Spherical	4.088 ± 0.062 hijk	4.084 ± 0.056 d	6.13221	14.823 ± 0.100 b	0.414
P. glabrum	MK-RSB26	OP411021.1	99.2 ± 0.37 ab	Spherical	2.884 ± 0.044 jk	2.912 ± 0.043 f	4.325355	11.782 ± 0.077 c	0.367
P. digitatum	MK-RSB10	OP411022.1	98.8 ± 0.20 ab	Spherical	2.824 ± 0.045 jk	2.834 ± 0.042 gf	4.236135	14.784 ± 0.051 b	0.287
Aspergillus niger	MK-RSB7	OP411015.1	99.0 ± 0.32 ab	Oval	4.317 ± 0.069 hij	4.050 ± 0.060 d	6.476145	10.190 ± 0.054 d	0.636
A. flavus	MK-RSB28	OP411016.1	99.0 ± 0.45 ab	Spherical	4.364 ± 0.072 hij	4.142 ± 0.059 d	6.54576	10.019 ± 0.207 d	0.653
Botrytis cinerea	MK-RSB24	OP411017.1	98.8 ± 0.37 ab	Ellipsoidal	7.934 ± 0.106 g	8.161 ± 0.116 b	11.90137	14.804 ± 0.066 b	0.804
Cladosporium cladosporioides	pc4	MK765911.1	99.0 ± 0.01 ab	Cylindrical	15.536 ± 0.278 e	2.587 ± 0.028 h	23.30463	14.718 ± 0.039 b	1.583
C. ramotenellum	AM55	MH259170.1	99.4 ± 0.40 a	Oval	12.399 ± 0.132 f	4.112 ± 0.052 d	18.59868	22.099 ± 0.219 a	0.842
C. limoniforme	Br15	MH245072.1	98.4 ± 0.24 ab	Cylindrical	4.655 ± 0.083 hi	1.802 ± 0.042 j	6.9828	14.790 ± 0.100 b	0.472
C. tenuissimum	K15	MH258971.1	99.2 ± 0.49 ab	Cylindrical	5.137 ± 0.055 h	2.092 ± 0.055 i	7.70484	14.759 ± 0.077 b	0.522
Fusarium oxysporum	7391	MK790682.1	98.8 ± 0.37 ab	Fusiform	8.765 ± 0.198 g	3.141 ± 0.055 e	13.14744	14.717 ± 0.091 b	0.893
F. proliferatum	pc91	MK765917.1	99.0 ± 0.32 ab	Fusiform	19.703 ± 0.317 d	2.667 ± 0.028 hg	29.55448	14.806 ± 0.066 b	1.996
F. solani	pc13	MK765916.1	98.2 ± 0.21 b	Fusiform	13.612 ± 0.347 f	4.112 ± 0.059 d	20.41795	14.895 ± 0.049 b	1.371
Alternaria alternata	MK-RSB6	OP411012.1	99.2 ± 0.20 ab	Obclavate	49.795 ± 1.761 a	8.582 ± 0.199 a	74.69284	11.680 ± 0.049 c	6.395
A. tenuissima	MK-RSB4	OP411013.1	99.2 ± 0.23 ab	Obclavate	29.929 ± 0.594 c	7.640 ± 0.145 e	44.89369	14.754 ± 0.090 b	3.043
A. arborescens	MK-RSB9	OP411014.1	98.6 ± 0.24 ab	Obclavate	34.556 ± 0.907 b	7.738 ± 0.145 e	51.83403	14.923 ± 0.077 b	3.473
Replicate			5		100	100		5	
Sum of squares			10.133		317496.495	8442.868		855.426	
df			20		20	20		20	
Mean square			0.507		15874.825	422.143		42.771	
F-value			0.917		711.693	645.758		845.531	
p-value			0.567		0.0001	0.0001		0.0001	

* Accession number of culture collection of agricultural microorganisms at Gorgan University of Agricultural Science and Natural Resources. ** Accession number of National Center for Biotechnology Information. *** One and a half times the spore length was considered as the final germination length and growth of the tube before branching and turning into the mycelia. The lowercase letters indicate groups based on Duncan's multiple range test.

PDB medium was then filtered through a 400-mesh filter to separate the mycelial and conidial biomass from the culture broth. An equal volume of analytical-grade ethyl acetate (Merck 109623) was added to the filtered PDB medium, and the mixture was incubated for 12 h at 25 ± 2 °C to ensure the inactivation of any remaining fungal components. The ethyl acetate was separated from the medium using a Buchner vacuum filtration funnel. The extracts were then evaporated at 60 °C using a rotary evaporator (Chemglass CG-1334-X64). The resulting extract was immediately diluted in 100 mL of HPLC analytical-grade n-hexane (Merck 104391) and either subjected to GC-MS analysis or stored at −20 °C in a laboratory-grade freezer (Thermo Fisher Scientific) until analysis.

Identification of secondary metabolites

The GC-MS analysis was conducted using an Agilent 7890A gas chromatograph interfaced with an Agilent 5975C mass spectrometer. The GC-MS system employed electron ionization at 70 eV. A non-polar capillary column (30 m × 0.25 mm i.d., 0.25 μm film thickness, DB-5MS or its equivalent) was utilized for chromatographic separation. A new and preconditioned DB-5MS column was used to ensure optimal performance and accuracy. The oven temperature was initially set to 60 °C for 1 min, followed by an increase of 10 °C/min until reaching 300 °C, where it was held for 5 min. The injector operated at 300 °C in splitless mode, and the detector temperature was maintained at 320 °C. Helium (99.99% purity, supplied by Linde Gas) served as the carrier gas, flowing at 1.0 mL/min. The mass spectrometer was set with an ion source temperature of 200 °C, scanning in the range of 35–450 m/z at a rate of 0.50 scans per second. A 3-min solvent delay was applied to avoid solvent-related interference.

The system was calibrated using a standard tuning mixture (PFTBA, perfluorotributylamine, Sigma-Aldrich), following the manufacturer's calibration guidelines. Metabolites were identified by comparing mass spectra against the National Institute of Standards and Technology (NIST) library version 23, with a match probability of ≥ 85%. Retention indices (RI) were calculated using a C8 –C40 n-alkane series (Sigma-Aldrich) run under the same conditions, and values were compared with literature data for further confirmation. Only compounds with ≥ 85% library match and consistent retention indices were considered positively identified. The identification was qualitative; no internal standard was used for absolute quantification. However, relative abundance was inferred from peak areas in the total ion chromatogram (TIC). Each sample, including both positive (caffeine) and negative (sterile media) controls, underwent triplicate injections.

Evaluation of the spore inhibition activity of secondary metabolites

The extract of each *Trichoderma* sp. was diluted in sterile PDB medium to achieve a concentration of 200 μg/mL. A sterile glass slide was placed in a sterile petri dish, followed by the addition of 1 mL of prepared PDB medium onto the slide. Subsequently, 100 μL of a post-harvest fungal pathogen spore suspension (10^5 spores/mL) was added onto the slide. The slide was covered with a sterile coverslip and incubated at 26 ± 2 °C with a relative humidity of 60% under dark conditions for 12 h. Spore germination was defined as the emergence of a visible germ tube that was at least half the diameter of the spore. After incubation, germination was assessed under a light microscope, and the percentage of germinated spores was calculated based on a count of 100 spores per replicate. The percentage of spore germination in PDB medium without secondary metabolites served as the control treatment (Table 1). Each experiment was conducted with five replicates, and the inhibition rate was calculated using the following formula:

$$\text{Inhibition rate (\%)} = \frac{\text{Gc} - \text{Gt}}{\text{Gc}} \times 100$$

where, Gc is the spore germination percentage in the control treatment, and Gt is the spore germination percentage in the presence of secondary metabolites extracted from Trichoderma species during the spore germination phase.

Statistical analysis

A completely randomized design was employed to investigate the impact of each *Trichoderma* sp. extract on the spore germination rate of postharvest plant pathogenic fungi. The collected data were analyzed using one-way analysis of variance (ANOVA). The Shapiro-Wilk test ($p < 0.05$) was used to assess the normality of data, and Levene's test ($p < 0.05$) was conducted to confirm the homogeneity of variances. ANOVA was performed using SPSS statistical software (Version 21.0, SPSS Inc., Chicago, IL, USA). Mean values of the treatments were compared using Duncan's multiple range test at $\alpha = 0.05$. Graphs were created using Microsoft Excel (Version 2211).

Results

Micromorphological characterization and germination dynamics of fungal spores

Microscopic evaluations revealed that the spore size of the fungi differed in terms of length, width, and shape, as detailed in Table 1. The highest and lowest spore length was recorded for *A. alternata* (49.795 μm) and *T. virens* (2.626 μm), respectively. In general, based on Duncan's multiple range test, *Trichoderma* spp., *Penicillium* spp., *Aspergillus* spp., *Cladosporium limoniforme*, and *C. tenuissimum* were grouped as fungi with spore lengths smaller than 5.2 μm, and no significant difference was observed among them. Approximately 42.85% of the other fungi exhibited a spore length greater than 7.9 μm. Furthermore, *A. alternata* had the largest spore width (8.58 μm), while *C. tenuissimum* had the smallest spore width (2.09 μm).

In terms of the end germination time, defined as the time when the length of the germination tube reaches one and a half times the length of the spore, species-specific differences were observed among the fungi in Table 1. *T. atroviride* and *T. harzianum* completed their germination period faster than the other species, taking approximately 8.7 and 8.8 h, respectively. *C. cladosporioides* exhibited the longest time (22 h) to complete spore germination. Approximately 61.90% of the studied fungi could complete the spore germination period within a time range exceeding 14 h. Only *T. virens*, *P. glabrum* and *A. alternata* completed the spore germination period within a time range of 11 to 12 h, and Duncan's multiple range test indicated a non-significant difference in germination time between these species. Additionally, *A. niger* and *A. flavus* exhibited a similar spore germination period, ranging from 10 to 11 h. By dividing the final length of the germination tube by the elapsed time, it was determined that *F. proliferatum*, *C. cladosporioides*, and *F. solani* showed the highest germination speeds, measuring 1.9, 1.5, and 1.3 μm/h, respectively. The lowest germination speed was observed in *P. digitatum*, with a rate of 0.287 μm/h. Among the *Trichoderma* species, *T. atroviride* exhibited the highest speed (0.681 μm/h), followed by *T. harzianum* (0.536 μm/h), and *T. virens* (0.334 μm/h).

Inhibitory effects of secondary metabolites on post-harvest pathogenic fungi

The inhibitory abilities of the secondary metabolites produced by each *Trichoderma* species varied among the post-harvest plant pathogenic fungi (Fig. 1). This ability displayed a notable distinction even in terms of inhibiting the spore germination of species within

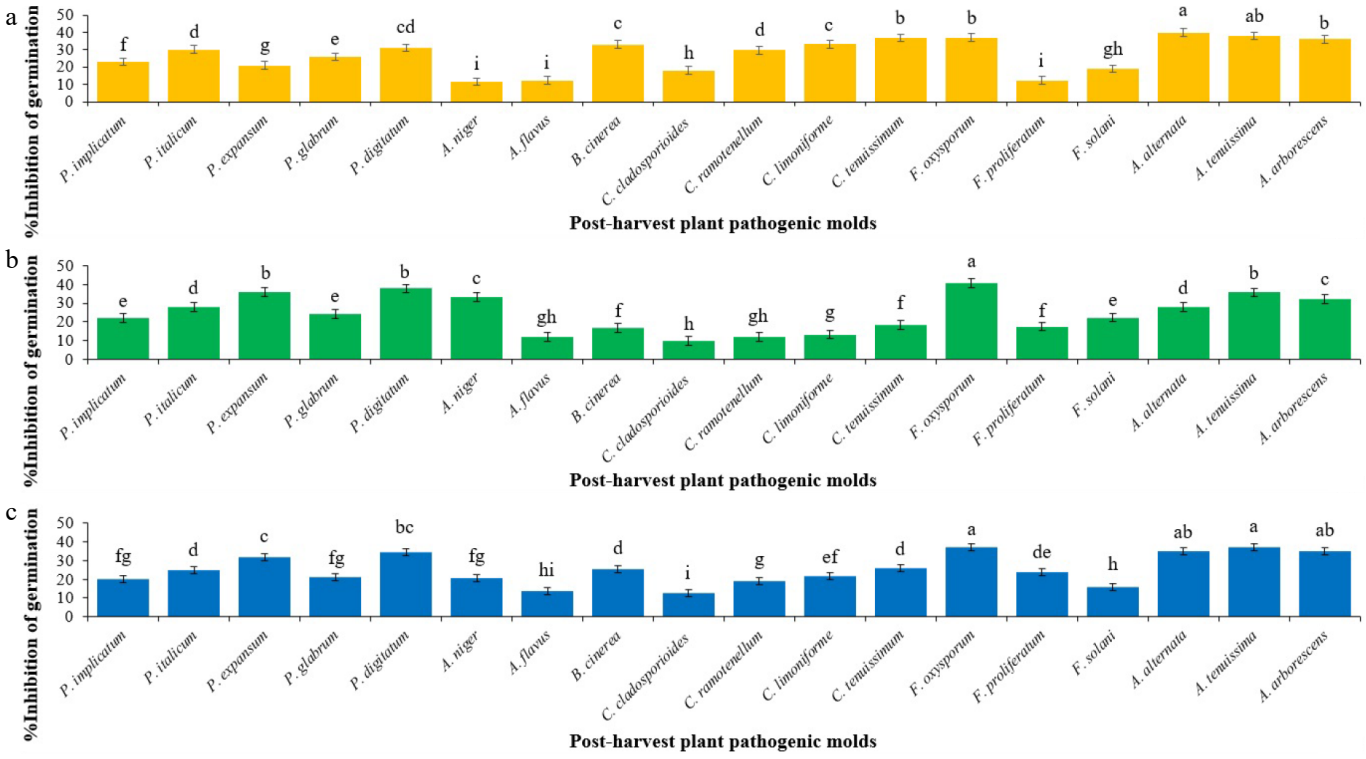

Fig. 1 Mean comparisons of the inhibition percentage of spore germination of post-harvest fungi as affected by secondary metabolites from initial spore germination stage of each *Trichoderma* sp. after 12 h. Values are means of five replicates. (a) The effect of *T. atroviride* on the inhibition of spore germination (Sum of squares: 7,659.592; df: 17; Mean square: 450.564; F-value: 169.764; *p*-value: 0.0001). (b) The effect of *T. harzianum* on the inhibition of spore germination (Sum of squares: 8316.157; df: 17; Mean square: 489.186; F-value: 142.419; *p*-value: 0.0001). (c) The effect of *T. virens* on the inhibition of spore germination (Sum of squares: 5410.919; df: 17; Mean square: 318.289; F-value: 86.543; *p*-value: 0.0001). Bars (standard error) with different letters indicate significant differences (Duncan range test subset for $\alpha = 0.05$).

the same genus. According to Duncan's multiple range test, the secondary metabolites of *T. atroviride* displayed the highest inhibitory effect on the spore germination of *A. alternata* and *A. tenuissima*, with 39.93% and 37.97%, respectively. No significant difference was observed between them (Fig. 1a). However, according to Duncan's multiple range test, the inhibitory ability of *T. atroviride* against the spore germination of *A. niger*, *A. flavus*, and *F. proliferatum* was grouped as the least effective treatments, and no significant difference observed between them (Fig. 1a). The secondary metabolites of *T. harzianum* exhibited the highest inhibitory ability against the spore germination of *F. oxysporum*, resulting in a reduction of 40.84% (Fig. 1b). On the other hand, the inhibitory capacity of *T. harzianum* secondary metabolites against the spore germination of *A. flavus*, *C. cladosporioides*, and *C. ramotenellum* reached a minimum level, and Duncan's multiple range test did not indicate a significant difference among them (Fig. 1b). Furthermore, the secondary metabolites of *T. virens* exhibited the highest inhibitory ability against the spore germination of *F. oxysporum*, *A. alternata*, *A. tenuissima*, and *A. arborescens*, resulting in reductions of 37.02%, 35.05%, 37.05%, and 35.06%, respectively. No significant difference was observed among these inhibitory effects (Fig. 1c). However, according to Duncan's multiple range test, the inhibitory effect of *T. virens* secondary metabolites against the spore germination of *C. cladosporioides* was classified as the least effective when compared to the other post-harvest plant pathogenic fungi (Fig. 1c).

In terms of grouping the inhibitory ability of the secondary metabolites of *Trichoderma* spp. against spore germination of a post-harvest pathogenic fungus (Fig. 2; Table 2), Duncan's multiple range test did not reveal any significant difference ($p > 0.05$) in inhibiting *A. flavus* and *A. tenuissima*. Secondary metabolites of *T. atroviride* showed the highest inhibitory ability against spore germination in 50% of the post-harvest plant pathogenic fungi, in comparison to *T. virens* and *T. harzianum*. However, *T. harzianum* revealed highest inhibitory ability against spore germination of *P. expansum, P. digitatum*, *A. niger*, *F. oxysporum*, *F. solani*, in comparison to *T. virens* and *T. atroviride*. Furthermore, secondary metabolites of *T. virens* only demonstrated the highest inhibitory ability against spore germination of *F. proliferatum* and *A. arborescens*, in comparison to *T. atroviride* and *T. harzianum*.

GC-MS profiling of secondary metabolites in *T. atroviride*

The results of GC-MS analysis revealed the presence of 23 secondary metabolites in the 12-h extract of PDB medium inoculated with *T. atroviride* spores, as detailed in Table 3 and illustrated in Fig. 3. The molecular weight of these secondary metabolites ranged from 86.134 g/mol (Pentanal) to 390.62 g/mol [1,4-Benzenedicarboxylic acid, bis(2-ethylhexyl) ester]. Secondary metabolites with a weight range between 200 and 300 g/mol exhibited the highest abundance, accounting for 43.47% of the identified metabolites from *T. atroviride*. Metabolites with a weight range between 100 and 200 g/mol followed, representing a frequency of 34.78%. Only four metabolites, accounting for 17.39% abundance, were detected in the molecular weight range between 300 and 400 g/mol in the 12-h extract of *T. atroviride*. Metabolites with a molecular weight range below 100 g/mol exhibited the lowest abundance, representing 4.34%. Furthermore, all the metabolites identified in the 12-h extract of *T. atroviride* was recorded for four chemical classes: simple hydrocarbons, organo-oxygens, organo-sulfurs, and organo-nitrogens. Among the identified metabolites, organo-oxygens and simple hydrocarbons were the most prevalent, accounting for 60.86 and

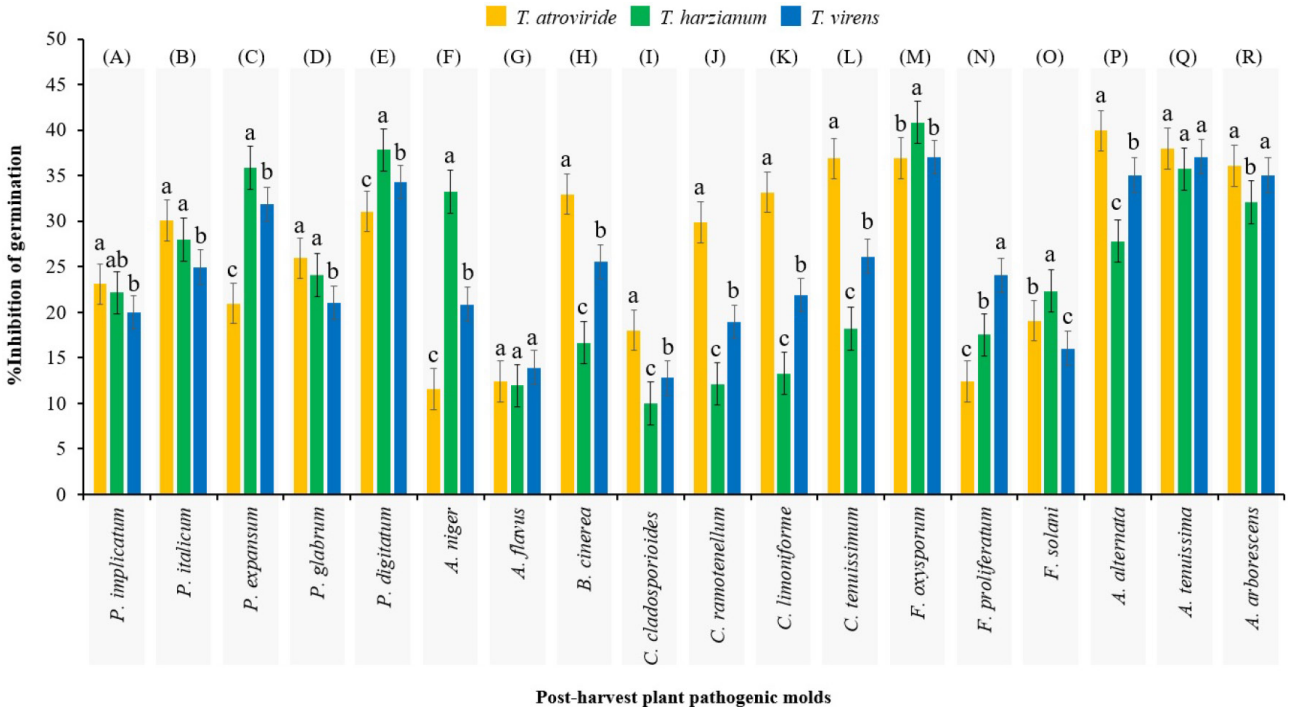

Fig. 2 Mean comparisons of the inhibition percentage of spore germination of each post-harvest fungus as affected by secondary metabolites from initial spore germination stage of *Trichoderma* spp. after 12 h. Values are means of five replicates. Bars (standard error) with different letters indicate significant differences. Sections (A)–(R) are independent experiments that grouped separately by Duncan's range test (subset for α = 0.05), which the results of their analysis of variance are presented in Table 2.

Table 2. Results of one-way analysis of variance (ANOVA) for duncan's multiple range test mean comparisons in Fig. 2.

Pathogenic post-harvest fungus	Analysis section	Sum of squares	df	Mean square	F-value	*p*-value
Penicillium implicatum	(A)	25.479	2	12.740	3.746	0.054
P. italicum	(B)	66.173	2	33.087	8.890	0.004
P. expansum	(C)	592.420	2	296.210	89.211	0.0001
P. glabrum	(D)	61.142	2	30.571	9.339	0.004
P. digitatum	(E)	114.723	2	57.361	18.508	0.0001
Aspergillus niger	(F)	1,178.349	2	589.174	191.312	0.0001
A. flavus	(G)	10.646	2	5.323	1.557	0.250
Botrytis cinerea	(H)	666.296	2	333.148	113.961	0.0001
Cladosporium cladosporioides	(I)	166.026	2	83.013	26.223	0.0001
C. ramotenellum	(J)	800.174	2	400.087	120.219	0.0001
C. limoniforme	(K)	993.039	2	496.519	159.835	0.0001
C. tenuissimum	(L)	878.684	2	439.342	147.069	0.0001
Fusarium oxysporum	(M)	49.905	2	24.952	6.971	0.010
F. proliferatum	(N)	341.754	2	170.877	49.327	0.0001
F. solani	(O)	98.872	2	49.436	16.515	0.0001
Alternaria alternata	(P)	373.321	2	186.660	54.973	0.0001
A. tenuissima	(Q)	12.768	2	6.384	2.014	0.176
A. arborescens	(R)	43.295	2	21.648	6.818	0.011

Not significant: *p*-value > 0.05; Significant: *p*-value < 0.05.

30.43%, respectively. Organic sulfurs and organo-nitrogens, on the other hand, exhibited the lowest frequency, each accounting for 4.34%. Among the metabolites, 1,4-Benzenedicarboxylic acid, bis(2-ethylhexyl) ester and 2-Hexanone, 5-methyl had the highest (47.78%) and lowest (0.11%) area percentages on the chromatogram graph, respectively.

Metabolite characterization of *T. virens* through GC-MS analysis

The quantity of secondary metabolites detected in the 12-h extract derived from PDB medium inoculated with *T. virens* spores was 9.52% lower compared to those found in *T. atroviride*, as detailed in Table 4 and illustrated in Fig. 3. GC-MS analysis revealed a total of 21 distinct secondary metabolites present in the extract of germinated *T. virens* spores. Among these compounds, 1,4-benzenedicarboxylic acid, bis(2-ethylhexyl) ester, demonstrated the highest chromatographic area percentage at 71.94%, whereas 2,4-di-tert-butylphenol exhibited the minimal relative abundance, registering only 0.02%. Notably, none of the metabolites identified within the 12-h *T. virens* extract possessed molecular weights below 100 g/mol. The most prevalent class of secondary metabolites fell within the molecular weight range of 100 to 200 g/mol, constituting 47.61% of the total detected compounds. This was followed by metabolites with molecular weights ranging from 200 to 300 g/mol,

Table 3. Details of the identified metabolites from initial spore germination stage of *Trichoderma atroviride*.

Peak no.	Metabolite	Time	Area	% Area	Molecular formula	Molecular weight (g/mol)	% Match against NIST*	CAS** registration no.
1	Pentanal	11.086	808690	0.8	$C_5H_{10}O$	86.134	78	110-62-3
2	2-Hexanone, 5-methyl	11.164	108673	0.11	$C_7H_{14}O$	114.185	78	110-12-3
3	Tridecane	14.64	13189397	12.97	$C_{13}H_{28}$	184.36	74	629-50-5
4	Dodecane	18.537	1456396	1.43	$C_{12}H_{26}$	170.34	94	112-40-3
5	Sulfurous acid, 2-propyl tridecyl ester	25.308	3418750	3.36	$C_{19}H_{40}O_3S$	348.59	95	309-12-4
6	4-Methylcyclohexanol	27.42	2268233	2.23	$C_7H_{14}O$	114.19	82	589-91-3
7	4-Methylheptane-3,5-dione	27.918	1917646	1.89	$C_8H_{14}O_2$	142.2	77	1187-04-8
8	5-Tridecanone	28.136	328445	0.32	$C_{13}H_{26}O$	198.34	76	30692-16-1
9	Lauric acid	28.281	492818	0.48	$C_{12}H_{24}O_2$	200.32	83	143-07-7
10	Margaric acid	28.38	702940	0.69	$C_{17}H_{34}O_2$	270.46	82	506-12-7
11	Pentane, 1-butoxy	28.427	254993	0.25	$C_9H_{20}O$	144.26	88	18636-66-3
12	Cytidine	28.551	429770	0.42	$C_9H_{13}N_3O_5$	243.22	76	65-46-3
13	1,5-anhydro-arabino-furanose	28.748	1292085	1.27	$C_5H_6O_3$	114.1	77	51246-91-4
14	Phenol, 2,4-bis(1,1-dimethylethyl)	28.878	3820885	3.76	$C_{14}H_{22}O$	206.33	96	96-76-4
15	Hexadecane	31.306	2198992	2.16	$C_{16}H_{34}$	226.44	96	544-76-3
16	1,1-Bis(p-tolyl)ethane	34.347	1348729	1.33	$C_{20}H_{22}$	262.39	91	98211-18-9
17	Octadecane	36.703	917085	0.9	$C_{18}H_{38}$	254.51	97	593-45-3
18	Palmitic acid, methyl ester	39.873	3225855	3.17	$C_{17}H_{34}O_2$	270.46	99	112-39-0
19	Benzenepropanoic acid, 3,5-bis(1,1-dimethylethyl)-4-hydroxy-, methyl ester	40.278	6285759	6.18	$C_{23}H_{36}O_3$	360.53	99	6386-38-5
20	Palmitic acid	40.822	6825347	6.71	$C_{16}H_{32}O_2$	256.42	99	57-10-3
21	Eicosane	41.603	859015	0.84	$C_{20}H_{42}$	282.56	94	112-95-8
22	Tetracosane	46.085	946504	0.93	$C_{24}H_{50}$	338.65	90	646-31-1
23	1,4-Benzenedicarboxylic acid, bis(2-ethylhexyl) ester	53.106	48578756	47.78	$C_{24}H_{38}O_4$	390.62	91	6422-86-2

* National Institute of Standards and Technology (version 23). ** Chemical Abstracts Service.

Table 4. Details of the identified metabolites from initial spore germination stage of *Trichoderma virens*.

Peak no.	Metabolite	Time	Area	% Area	Molecular formula	Molecular weight (g/mol)	% Match against NIST*	CAS** registration no.
1	2-Hexanone, 5-methyl	11.045	1308158	0.73	$C_7H_{14}O$	114.19	80	110-12-3
2	Propene, 1,1'-oxybis	11.081	140978	0.08	$C_6H_{12}O$	100.16	78	4696-29-1
3	5-Methyluracil	14.666	14678214	8.19	$C_5H_6N_2O_2$	126.11	80	65-71-4
4	Dodecane	18.532	1324048	0.74	$C_{12}H_{26}$	170.34	94	112-40-3
5	Tetradecane	25.303	3020121	1.68	$C_{14}H_{30}$	198.41	94	629-59-4
6	d-Lyxo-d-manno-nononic-1,4-lactone	27.322	559198	0.31	$C_9H_{16}O_9$	268.22	72	3080-49-7
7	5-Tridecanone	27.467	515994	0.29	$C_{13}H_{26}O$	198.34	74	30692-16-1
8	1,5-anhydro-arabino-furanose	27.591	402534	0.22	$C_5H_6O_3$	114.1	83	51246-91-4
9	Undecanoic acid	28.38	706513	0.39	$C_{11}H_{22}O_2$	186.29	87	112-37-8
10	Pentane, 1-butoxy	28.458	106359	0.06	$C_9H_{20}O$	144.26	83	18636-66-3
11	2,4-Di-tert-butylphenol	28.51	37983	0.02	$C_{14}H_{22}O$	206.32	83	96-76-4
12	Decanoic acid	28.878	4084001	2.28	$C_{10}H_{20}O_2$	172.26	96	112-37-8
13	Hexadecane	31.306	2051964	1.14	$C_{16}H_{34}$	226.44	96	544-76-3
14	1,1-Bis(p-tolyl)ethane	34.347	1583496	0.88	$C_{16}H_{18}$	210.31	90	98211-18-9
15	Octadecane	36.703	762932	0.43	$C_{18}H_{38}$	254.51	95	593-45-3
16	Hexadecanoic acid, methyl ester	39.868	2090101	1.17	$C_{17}H_{34}O_2$	270.45	98	112-39-0
17	Benzenepropanoic acid, 3,5-bis(1,1-dimethylethyl)-4-hydroxy-, methyl ester	40.278	6308220	3.52	$C_{14}H_{20}O_3$	236.31	99	6386-38-5
18	Palmitic acid	40.796	2276043	1.27	$C_{16}H_{32}O_2$	256.42	99	57-10-3
19	2-methyloctacosane	46.084	838744	0.47	$C_{29}H_{60}$	408.8	90	1560-98-1
20	1,4-Benzenedicarboxylic acid, bis(2-ethylhexyl) ester	53.138	128988610	71.94	$C_{24}H_{38}O_4$	390.62	91	422-86-2
21	Phthalic acid, di(2-propylphenyl) ester	56.669	7520123	4.19	$C_{26}H_{26}O_4$	402.5	94	98661-89-0

* National Institute of Standards and Technology (version 23). ** Chemical Abstracts Service.

which represented the second most abundant category. Conversely, compounds with molecular masses between 300 to 400 g/mol and 400 to 500 g/mol were comparatively scarce, comprising 9.52% and 4.78%, respectively. Among the metabolites characterized, 2-methyloctacosane exhibited the greatest molecular weight at 408.8 g/mol, while Propene, 1,1'-oxybis was the lightest, at 100.16 g/mol. Interestingly, no organo-sulfur compounds were detected in the extract. The chemical class of organo-oxygen compounds dominated the profile, accounting for 66.66% of the metabolites identified, followed by simple hydrocarbons which constituted 28.57%. Only a single metabolite belonging to the organo-nitrogen class was present within the 12-h *T. virens* extract.

Table 5. Details of the identified metabolites from initial spore germination stage of *Trichoderma harzianum*.

Peak no.	Metabolite	Time	Area	% Area	Molecular formula	Molecular weight (g/mol)	% Match against NIST*	CAS** registration no.
1	2,4-Diamino-6-hydroxypyrimidine	14.614	3064400	3.39	$C_4H_6N_4O$	126.12	64	56-06-4
2	Dodecane	18.532	1314498	1.45	$C_{12}H_{26}$	170.34	95	112-40-3
3	Tetradecane	25.303	2574175	2.84	$C_{14}H_{30}$	198.41	94	629-59-4
4	2-Vinyl-9-[beta-d-ribofuranosyl]hypoxanthine	27.446	2051010	2.27	$C_{12}H_{14}N_4O_5$	294.26	77	110851-56-4
5	5-Tridecanone	27.524	209944	0.23	$C_{13}H_{26}O$	198.34	75	30692-16-1
6	1,5-anhydro-arabino-furanose	27.737	473868	0.52	$C_5H_6O_3$	114.1	72	51246-91-4
7	Itaconic acid	27.788	85858	0.09	$C_5H_6O_4$	130.09	85	97-65-4
8	Cyclopentanol	27.892	96554	0.11	$C_5H_{10}O$	86.1323	87	96-41-3
9	2,4-Di-tert-butylphenol	28.878	1984097	2.19	$C_{14}H_{22}O$	206.32	96	96-76-4
10	Hexadecane	31.306	1866061	2.06	$C_{16}H_{34}$	226.44	98	544-76-3
11	1,1-Bis(p-tolyl)ethane	34.347	1533054	1.69	$C_{16}H_{18}$	210.31	91	98211-18-9
12	Octadecane	36.697	1005421	1.11	$C_{18}H_{38}$	254.51	96	593-45-3
13	Hexadecanoic acid, methyl ester	39.873	2703467	2.99	$C_{17}H_{34}O_2$	270.45	98	112-39-0
14	Benzenepropanoic acid, 3,5-bis(1,1-dimethylethyl)-4-hydroxy-, methyl ester	40.277	6624034	7.32	$C_{14}H_{20}O_3$	236.31	99	6386-38-5
15	Palmitic acid	40.802	2434738	2.69	$C_{16}H_{32}O_2$	256.42	99	57-10-3
16	Icosane	41.606	2069726	2.29	$C_{20}H_{42}$	282.54	97	112-95-8
17	2-methyloctacosane	46.089	1568284	1.73	$C_{29}H_{60}$	408.8	98	1560-98-1
18	Heneicosane, 11-(1-ethylpropyl)	50.214	846188	0.94	$C_{26}H_{54}$	366.7	87	55282-11-6
19	Phthalic acid, di(2-propylpentyl) ester	53.088	13204422	14.59	$C_{26}H_{26}O_4$	402.5	91	998661-89-0
20	1,4-Benzenedicarboxylic acid, bis(2-ethylhexyl) ester	56.684	44774953	49.48	$C_{24}H_{38}O_4$	390.62	94	6422-86-2

* National Institute of Standards and Technology (version 23). ** Chemical Abstracts Service.

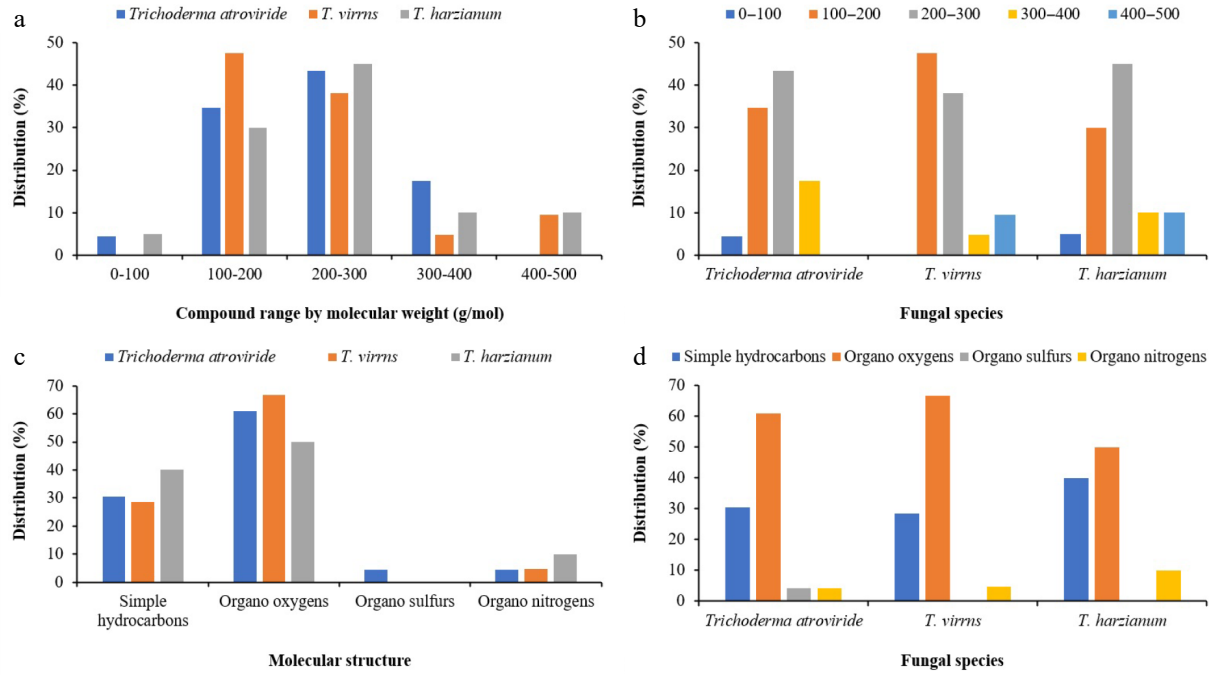

Fig. 3 Clustered column charts illustrating the distribution percentages of various metabolites across *Trichoderma* spp. extracts based on GC-MS analysis. (a) and (b) represent the distribution percentages categorized by molecular weight. (c) and (d) display the distribution percentages classified by molecular structure.

Characterization of secondary metabolites from *T. harzianum* extract

According to the data presented in Table 5 and Fig. 3, the quantity of secondary metabolites detected during the initial spore germination phase of *T. harzianum* was 15% and 5% lower than that observed in *T. atroviride* and *T. virens*, respectively. Nonetheless, the molecular weight distribution of the metabolites identified in *T. harzianum* exhibited greater heterogeneity compared to the other two species. Overall, GC-MS analysis revealed the presence of 20 secondary metabolites in the 12-h extract of PDB medium inoculated with *T. harzianum* spores. Among these, only Cyclopentanol was characterized by a molecular weight below 100 g/mol. The most prevalent metabolites fell within the 200 to 300 g/mol and 100 to 200 g/mol weight intervals, constituting approximately 45% and 30% of the total compounds identified, respectively. Metabolites with molecular weights ranging from 300 to 400 g/mol and 400 to 500 g/mol were equally represented, each comprising 10% of the total profile. The heaviest compound identified was

2-methyloctacosane, with a molecular mass of 408.8 g/mol. On the chromatographic profile, 1,4-benzenedicarboxylic acid, bis(2-ethylhexyl) ester accounted for the greatest relative abundance (49.48%), whereas Cyclopentanol was the least abundant, registering only 0.11%. Chemically, organo-oxygen compounds dominated the metabolite spectrum at 50%, followed closely by simple hydrocarbons at 40%. Notably, organo-sulfur compounds were absent from the metabolite profile of *T. harzianum* at this stage, while organo-nitrogen compounds were detected at a comparatively lower frequency of 10%.

Discussion

The results demonstrate that the secondary metabolites derived from the initial spore germination stage of *Trichoderma* spp. actively inhibit the spore germination of all post-harvest plant pathogenic fungi. On average, *T. atroviride*, *T. harzianum*, and *T. virens* exhibited inhibitory activities of 27%, 24%, and 25%, respectively, against spore germination of 18 post-harvest fungal pathogens. According to the literature, secondary metabolites derived from the mycelial growth stage of *Trichoderma* spp. have shown efficacy against *Penicillium* spp.[18,20], *Aspergillus* spp.[14,15,20], *B. cinerea*[20–22], *Cladosporium* spp.[20,23], *Fusarium* spp.[15,20,24–26], and *Alternaria* spp.[27,28]. Although these studies, in line with our findings, highlight the significant bioactivity of *Trichoderma* spp. metabolites, none have investigated the compounds produced specifically during the spore germination stage.

This study provides the first evidence that spore germination metabolites of *Trichoderma* spp. serve as key competitive factors in the environment, enabling rapid niche colonization and suppression of competing spores before hyphal establishment, thereby positioning *Trichoderma* spp. as early ecological dominants in microhabitats. GC-MS analysis identified 39 secondary metabolites produced by *T. harzianum*, *T. virens*, and *T. atroviride* during this early developmental stage. Of these, 30.76% were unique to *T. atroviride*, while 12.82% and 15.38% were specifically produced by *T. virens* and *T. harzianum*, respectively. Additionally, 23.07% of the compounds were shared across all three species. Another 12.82% were common to *T. virens* and *T. harzianum*, whereas only 5.12% were shared between *T. atroviride* and *T. virens*. These early-stage *Trichoderma* metabolites show potential for biocontrol, particularly in postharvest settings where fungal spores are present but mycelial growth hasn't begun.

Diversity of initial spore germination stage metabolites of *Trichoderma* spp.

Several metabolites identified in this study have previously demonstrated antimicrobial activity during the mycelial growth stage of *Trichoderma* spp. For example, we exclusively detected lauric acid in *T. atroviride*, a compound that has also been reported during the mycelial stage of *T. atroviride*, *T. harzianum*, and *T. asperellum*[29–31]. Studies have confirmed that monolaurin, a derivative of lauric acid, inhibits various fungal species, including *Candida albicans*[32] and *Trichophyton rubrum*[33]. Researchers attribute this antifungal activity to monolaurin's ability to disrupt fungal lipid membranes, leading to cell lysis and death[34]. We also identified palmitic acid, methyl ester exclusively from *T. atroviride*, which belongs to the class of fatty acid methyl esters (FAMEs). Studies have shown that FAMEs derived from vegetable oils exhibit antifungal activity against pathogens such as *Paracoccidioides* spp., *C. glabrata*, *C. krusei*, and *C. parapsilosis*[35]. Additionally, FAMEs extracted from *Sesuvium portulacastrum* leaves have demonstrated antimicrobial effects against both bacterial and fungal human pathogens[36]. The production of palmitic acid and its methyl ester has also been observed during the mycelial stage of *T. longibrachiatum* and *T. reesei*[37,38]. Palmitic acid was also detected in all *Trichoderma* species examined in this study. *In vitro* experiments have revealed that palmitic acid effectively inhibits *C. tropicalis* and its biofilm formation, a critical factor in fungal pathogenicity[39]. Previous research has reported the biosynthesis of palmitic acid during the mycelial phase of *T. virens* and *T. harzianum*[16].

We identified undecanoic acid exclusively during the spore germination stage of *T. virens*. However, prior studies have reported this metabolite during the mycelial stage of *T. harzianum*, *T. koningii*, *T. koningiopsis*, and *T. asperellum*[31,40–42]. Rossi et al.[43] highlighted undecanoic acid's potential as a therapeutic antifungal agent. Similarly, the study of Lee et al.[44] demonstrated its ability to interfere with fungal communication and exert antibiofilm and anti-virulence effects against *C. albicans*. Moreover, Avrahami & Shai[45] explained that conjugating undecanoic acid with amino acid-containing antimicrobial peptides enhanced their antifungal activity. Although earlier studies have identified decanoic acid during the mycelial stage of *T. viride*, *T. koningii*, *T. koningiopsis*, *T. reesei*, and *T. virens*[40,46–48], we detected it only during the spore germination stage of *T. virens*.

The antifungal mechanism of decanoic acid is believed to involve membrane disruption, causing cellular leakage and fungal cell death[49]. Itaconic acid was uniquely detected in *T. harzianum* in this research, whereas previous studies have reported its presence during the mycelial stage of *T. reesei*[50]. Itaconic acid has been found to exert anti-inflammatory and antibacterial effects[51]. Multiple studies have explored itaconic acid's antimicrobial roles in macrophages and its function as an endogenous antimicrobial metabolite[52]. A study reported the antibacterial activities of hexadecanoic acid methyl ester against multidrug-resistant bacteria[53]. We also identified hexadecanoic acid, methyl ester similar from *T. virens* and *T. harzianum*, which is commonly referred to as methyl palmitate and has been isolated from the mycelial stage of *T. pseudokoningii*[17,20]. Differences in metabolite profiles between germination and mycelial stages suggest that *Trichoderma* probably regulates secondary metabolism in a phase-specific manner, likely influenced by environmental and developmental signals, an area worth further study.

Metabolites without an antifungal background

Several metabolites identified during the initial spore germination stage of *Trichoderma* spp. in this study, as well as those reported during the mycelial phase in previous investigations, have not been shown to possess direct antifungal activity. For example, we exclusively detected tridecane in *T. atroviride* during spore germination, although Siddiquee et al.[19] previously reported it during the mycelial stage of the same species. Similarly, we identified dodecane during the spore germination stage of all *Trichoderma* spp., while earlier studies have documented its presence only during the mycelial phase of *T. harzianum*[29]. Phenol, 2,4-bis(1,1-dimethylethyl), was detected exclusively in *T. atroviride* in our current analysis, whereas Mulatu et al.[54] found this compound in the mycelial stage of *T. asperellum* and *T. longibrachiatum*. Although we identified hexadecane in *T. atroviride*, *T. harzianum*, and *T. asperellum*, previous literature has confirmed its occurrence only in the mycelial stage of *T. harzianum*[55]. In alignment with our findings, the literature also confirms that octadecane appears commonly in both spore germination and mycelial stages of *T. atroviride*, *T. harzianum*, and *T. virens*[56,57].

We exclusively identified eicosane during the spore germination stage of *T. atroviride*, while earlier studies reported this compound

only in the mycelial phase of *T. harzianum*[58]. Furthermore, literature findings indicate that tetradecane occurs during the mycelial stage of *T. biocontroller*, *T. harzianum*, *T. viride*, *T. asperellum*, and *T. virens*[59–61]. However, we detected it during the spore germination stage of *T. virens* and *T. harzianum*. Both phthalic acid, di(2-propylphenyl) ester and 2,4-Di-tert-butylphenol were identified in the spore germination stage of *T. virens* and *T. harzianum* in this study. In contrast, previous reports have described phthalic acid, di(2-propylphenyl) ester only during the mycelial stage of *T. pinnatum*[62], and 2,4-Di-tert-butylphenol from *T. asperellum*[63]. Consistent with our results, the literature also confirms the presence of 2,4-diamino-6-hydroxypyrimidine in both the spore germination and mycelial phases of *T. harzianum*[64]. Importantly, 56.41% of the metabolites identified in this study have not been previously reported in any *Trichoderma* species. However, the study is limited to extracellular compounds and spore germination assays. Future research should explore metabolite synergy, molecular regulation, broader pathogen targets, and real-world efficacy.

Conclusions

These findings elucidate the crucial role of these metabolites in mediating the initial competitive interactions of *Trichoderma* spp. with other fungi, thereby enhancing their dominance in the environment. By unraveling the ecological significance of these metabolites in *Trichoderma* interactions with other organisms and the surrounding environment, our study contributes to a deeper understanding of microbial ecology and secondary metabolite biology. Importantly, these insights also have practical implications for postharvest disease management. The early production of antifungal metabolites suggests that *Trichoderma* spp. can be strategically employed to suppress pathogenic fungi during vulnerable postharvest stages. Understanding the timing and profile of metabolite release may inform the development of more effective biocontrol formulations, enabling targeted application to reduce spoilage and losses in storage and supply chains.

Ethical statements

This research did not involve any studies with human participants, and no ethical approval was required according to the institutional and national regulations.

Authors contributions

All authors contributed to the study's conception and design. Kamran Rahnama contributed to conceptualization, funding acquisition, methodology, project administration, resources, supervision, validation, visualization, writing – review and editing. Nima Akbari Oghaz contributed to conceptualization, data curation, formal analysis, investigation, software, validation, visualization, and writing of the original draft. Nooshin Drakhshan contributed to conceptualization, data curation, investigation, validation, visualization, writing – review and editing. Ruvishika Shehali Jayawardena contributed to conceptualization, formal analysis, validation, visualization, writing – review and editing. All participating authors read, commented, and approved the current version of the manuscript.

Data availability

Raw data supporting the findings of this study are available from the corresponding author upon reasonable request. The genome sequences and related information of utilized fungi in this research project are available online at the GenBank Nucleotide database of the National Center for Biotechnology Information (www.ncbi.nlm.nih.gov).

Acknowledgments

This study was an intra-academic research project of Gorgan University of Agricultural Sciences and Natural Resources under the supervision of Prof. Dr. Kamran Rahnama. The authors thank for Dr. Kevin David Hyde (Professor at Center of Excellence in Fungal Research, Mae Fah Luang University) for valuable scientific advice during this research project. This work was financially supported by Gorgan University of Agricultural Sciences and Natural Resources (Grant No. 00-45-666).

Conflict of interest

The authors declare that they have no conflict of interest.

Dates

Received 30 January 2025; Revised 30 June 2025; Accepted 1 July 2025; Published online 8 August 2025

References

1. Liu J, Sui Y, Wisniewski M, Xie Z, Liu Y, et al. 2018. The impact of the postharvest environment on the viability and virulence of decay fungi. *Critical Reviews in Food Science and Nutrition* 58:1681–87
2. Navale V, Vamkudoth KR, Ajmera S, Dhuri V. 2021. *Aspergillus* derived mycotoxins in food and the environment: prevalence, detection, and toxicity. *Toxicology Reports* 8:1008–30
3. Abramson D. 2020. Toxicants of the genus *Penicillium*. In *Handbook of plant and fungal toxicants*, ed. D'Mello JPF. 1st Edition. Boca Raton: CRC Press. pp. 303–17. doi: 10.1201/9780429281952-21
4. Bi K, Liang Y, Mengiste T, Sharon A. 2022. Killing softly: a roadmap of *Botrytis cinerea* pathogenicity. *Trends in Plant Science* 28:211–22
5. Summerell BA. 2019. Resolving *Fusarium*: current status of the genus. *Annual Review Of Phytopathology* 57:323–39
6. Aichinger G, Del Favero G, Warth B, Marko D. 2021. Alternaria toxins—still emerging? *Comprehensive Reviews in Food Science and Food Safety* 20:4390–406
7. Oghaz NA, Hatamzadeh S, Rahnama K, Moghaddam MK, Vaziee S, et al. 2022. Adjustment and quantification of UV–visible spectrophotometry analysis: an accurate and rapid method for estimating *Cladosporium* spp. spore concentration in a water suspension. *World Journal of Microbiology and Biotechnology* 38:183
8. Oyom W, Li YC, Prusky D, Zhang Z, Bi Y, et al. 2022. Recent advances in postharvest technology of Asia pears fungi disease control: A review. *Physiological and Molecular Plant Pathology* 117:101771
9. Rani L, Thapa K, Kanojia N, Sharma N, Singh S, et al. 2021. An extensive review on the consequences of chemical pesticides on human health and environment. *Journal of Cleaner Production* 283:124657
10. Corkley I, Fraaije B, Hawkins N. 2022. Fungicide resistance management: maximizing the effective life of plant protection products. *Plant Pathology* 71:150–69
11. Jahantigh S, Oghaz NA, Rahnama K, Hatamzadeh S. 2023. Application of *Lactobacillus* spp. for the biological management of green mold (*Penicillium digitatum*) on sweet orange fruit under *in vitro* and storehouse conditions. *Biocontrol Science and Technology* 33:567–81
12. Hatamzadeh S, Akbari Oghaz N, Rahnama K, Noori F. 2024. Comparison of the antifungal activity of chlorine dioxide, peracetic acid and some chemical fungicides in post-harvest management of *Penicillium digitatum* and *Botrytis cinerea* infecting sweet orange and strawberry fruits. *Agricultural Research* 13:72–84
13. Oghaz NA, Rahnama K, Habibi R, Razavi SI, Farias ARG. 2024. Endophytic and rhizospheric *Trichoderma* spp. associated with cucumber plants as

potential biocontrol agents of *Fusarium oxysporum* f. sp. *cucumerinum*. *Asian Journal of Mycology* 7:31–46
14. Guzmán-Guzmán P, Kumar A, de Los Santos-Villalobos S, Parra-Cota FI, Orozco-Mosqueda MdC, et al. 2023. *Trichoderma* species: our best fungal allies in the biocontrol of plant diseases—a review. *Plants* 12:432
15. Schuster A, Schmoll M. 2010. Biology and biotechnology of *Trichoderma*. *Applied Microbiology and Biotechnology* 87:787–99
16. Dubey SC, Tripathi A, Dureja P, Grover A. 2011. Characterization of secondary metabolites and enzymes produced by *Trichoderma* species and their efficacy against plant pathogenic fungi. *Indian Journal of Agricultural Sciences* 81:455–61
17. Khan IH, Javaid A. 2020. In vitro biocontrol potential of *Trichoderma pseudokoningii* against *Macrophomina phaseolina*. *International Journal of Agriculture and Biology* 24:730–36
18. Zhang JL, Tang WL, Huang QR, Li YZ, Wei ML, et al. 2021. Trichoderma: a treasure house of structurally diverse secondary metabolites with medicinal importance. *Frontiers in Microbiology* 12:723828
19. Siddiquee S, Cheong BE, Taslima K, Kausar H, Hasan MM. 2012. Separation and identification of volatile compounds from liquid cultures of *Trichoderma harzianum* by GC-MS using three different capillary columns. *Journal of Chromatographic Science* 50:358–67
20. Khan RAA, Najeeb S, Hussain S, Xie B, Li Y. 2020. Bioactive secondary metabolites from *Trichoderma* spp. against phytopathogenic fungi. *Microorganisms* 8:817
21. Risoli S, Cotrozzi L, Sarrocco S, Nuzzaci M, Pellegrini E, et al. 2022. Trichoderma-induced resistance to *Botrytis cinerea* in *Solanum* species: a meta-analysis. *Plants* 11:180
22. Vos CMF, De Cremer K, Cammue BPA, De Coninck B. 2015. The toolbox of *Trichoderma* spp. in the biocontrol of *Botrytis cinerea* disease. *Molecular Plant Pathology* 16:400–12
23. Barbosa MAG, Rehn KG, Menezes M, de Lima R Mariano R. 2001. Antagonism of *Trichoderma* species on *Cladosporium herbarum* and their enzimatic characterization. *Brazilian Journal of Microbiology* 32:98–104
24. Mironenka J, Różalska S, Soboń A, Bernat P . 2021. *Trichoderma harzianum* metabolites disturb *Fusarium culmorum* metabolism: metabolomic and proteomic studies. *Microbiological Research* 249:126770
25. Modrzewska M, Błaszczyk L, Stępień Ł, Urbaniak M, Waśkiewicz A, et al. 2022. *Trichoderma* versus *Fusarium*—inhibition of pathogen growth and mycotoxin biosynthesis. *Molecules* 27:8146
26. Sharma IP, Sharma AK. 2020. *Trichoderma–Fusarium* interactions: a biocontrol strategy to manage wilt. In *Trichoderma: Host pathogen interactions and applications*, ed. Sharma A, Sharma P. Singapore: Springer. pp. 167–85. doi: 10.1007/978-981-15-3321-1_9
27. Metz N, Hausladen H. 2022. *Trichoderma* spp. as potential biological control agent against *Alternaria solani* in potato. *Biological Control* 166:104820
28. Shafique S, Shafique S, Javed A, Akhtar N, Bibi S. 2019. Analysis of antagonistic potential of secondary metabolites and organic fractions of *Trichoderma* species against *Alternaria Alternata*. *Biocontrol Science* 24:81–88
29. Carratore RD, Gervasi PG, Contini MP, Beffy P, Maserti BE, et al. 2011. Expression and characterization of two new alkane-inducible cytochrome P450s from *Trichoderma harzianum*. *Biotechnology Letters* 33:1201–6
30. Liu XH, Song YP, Wang BG, Ji NY. 2021. Sesquiterpenes and lipids from the algicolous fungus *Trichoderma atroviride* RR-dl-3-9. *Phytochemistry Letters* 45:6–12
31. Zhang XF, Li QY, Wang M, Ma SQ, Zheng YF, et al. 2022. 2*E*,4*E*-decadienoic acid, a novel anti-oomycete agent from coculture of *Bacillus subtilis* and *Trichoderma asperellum*. *Microbiology Spectrum* 10:e01542-22
32. Ogbolu DO, Oni AA, Daini OA, Oloko AP. 2007. In vitro antimicrobial properties of coconut oil on *Candida species* in Ibadan, Nigeria. *Journal of Medicinal Food* 10:384–87
33. Tsuji Y, Torti SV, Torti FM. 1998. Activation of the ferritin H enhancer, FER-1, by the cooperative action of members of the AP1 and Sp1 transcription factor families. *Journal of Biological Chemistry* 273:2984–92
34. Walsh M, Whitlock R, Garg AX, Légaré JF, Duncan AE, et al. 2016. Effects of remote ischemic preconditioning in high-risk patients undergoing cardiac surgery (Remote IMPACT): a randomized controlled trial. *CMAJ* 188:329–36
35. Pinto MEA, Araújo SG, Morais MI, Sá NP, Lima CM, et al. 2017. Antifungal and antioxidant activity of fatty acid methyl esters from vegetable oils. *Anais da Academia Brasileira de Ciências* 89:1671–81
36. Chandrasekaran M, Senthilkumar A, Venkatesalu V. 2011. Antibacterial and antifungal efficacy of fatty acid methyl esters from the leaves of Sesuvium portulacastrum L. *European Review for Medical and Pharmacological Sciences* 15:775–80
37. Brown DE, Hasan M, Lepe-Casillas M, Thornton AJ. 1990. Effect of temperature and pH on lipid accumulation by *Trichoderma reesei*. *Applied Microbiology and Biotechnology* 34:335–39
38. Ruiz N, Dubois N, Wielgosz-Collin G, du Pont TR, Bergé JP, et al. 2007. Lipid content and fatty acid composition of a marine-derived *Trichoderma longibrachiatum* strain cultured by agar surface and submerged fermentations. *Process Biochemistry* 42:676–80
39. Prasath KG, Tharani H, Kumar MS, Pandian SK. 2020. Palmitic acid inhibits the virulence factors of *Candida tropicalis*: biofilms, cell surface hydrophobicity, ergosterol biosynthesis, and enzymatic activity. *Frontiers in Microbiology* 11:864
40. Chahal A, Monreal CM, Bissett J, Rowland O, Smith ML, et al. 2014. Metabolism of n-C10:0 and n-C11:0 fatty acids by *Trichoderma koningii, Penicillium janthinellum* and their mixed culture: I. Biomass and CO_2 production, and allocation of intracellular lipids. *Journal of Environmental Science and Health, Part B* 49:945–54
41. Serrano-Carreon L, Hathout Y, Bensoussan M, Belin JM. 1992. Production of 6-pentyl-α-pyrone by *Trichoderma harzianum* from 18: n fatty acid methyl esters. *Biotechnology Letters* 14:1019–24
42. Sreenayana B, Vinodkumar S, Nakkeeran S, Muthulakshmi P, Poornima K. 2022. Multitudinous potential of *Trichoderma* species in imparting resistance against *F. oxysporum* f. sp. cucumerinum and *Meloidogyne incognita* disease complex. *Journal of Plant Growth Regulation* 41:1187–206
43. Rossi A, Martins MP, Bitencourt TA, Peres NTA, Rocha CHL, et al. 2021. Reassessing the use of undecanoic acid as a therapeutic strategy for treating fungal infections. *Mycopathologia* 186:327–40
44. Lee JH, Kim YG, Khadke SK, Lee J. 2021. Antibiofilm and antifungal activities of medium-chain fatty acids against Candida albicans via mimicking of the quorum-sensing molecule farnesol. *Microbial Biotechnology* 14:1353–66
45. Avrahami D, Shai Y. 2003. Bestowing antifungal and antibacterial activities by lipophilic acid conjugation to D,L-amino acid-containing antimicrobial peptides: a plausible mode of action. *Biochemistry* 42:14946–56
46. Angel LPL, Sundram S, Ping BTY, Yusof MT, Ismail IS. 2018. Profiling of anti-fungal activity of *Trichoderma virens* 159C involved in biocontrol assay of *Ganoderma boninense*. *Journal of Oil Palm Research* 30:83–93
47. Collins RP, Halim AF. 1972. Characterization of the major aroma constituent of the fungus *Trichoderma viride*. *Journal of Agricultural and Food Chemistry* 20:437–38
48. Huang R, Zhang F, Zhou H, Yu H, Shen L, et al. 2023. Characterization of *Trichoderma reesei* endoglucanase displayed on the *Saccharomyces cerevisiae* cell surface and its effect on wine flavor in combination with β-glucosidase. *Process Biochemistry* 124:140–49
49. Kabara JJ, Swieczkowski DM, Conley AJ, Truant JP. 1972. Fatty acids and derivatives as antimicrobial agents. *Antimicrobial Agents and Chemotherapy* 2:23–28
50. Schlembach I, Hosseinpour Tehrani H, Blank LM, Büchs J, Wierckx N, et al. 2020. Consolidated bioprocessing of cellulose to itaconic acid by a co-culture of *Trichoderma reesei* and *Ustilago maydis*. *Biotechnology for Biofuels* 13:207
51. Teleky B-E, Vodnar DC. 2021. Recent advances in biotechnological itaconic acid production, and application for a sustainable approach. *Polymers* 13:3574
52. Cordes T, Michelucci A, Hiller K. 2015. Itaconic acid: the surprising role of an industrial compound as a mammalian antimicrobial metabolite. *Annual Review of Nutrition* 35:451–73
53. Shaaban MT, Ghaly MF, Fahmi SM. 2021. Antibacterial activities of hexadecanoic acid methyl ester and green-synthesized silver

nanoparticles against multidrug-resistant bacteria. *Journal of basic microbiology* 61:557–68

54. Mulatu A, Megersa N, Tolcha T, Alemu T, Vetukuri RR. 2022. Antifungal compounds, GC-MS analysis and toxicity assessment of methanolic extracts of *Trichoderma* species in an animal model. *PLoS One* 17:e0274062
55. Serrano-Carreón L, Balderas-Ruíz K, Galindo E, Rito-Palomares M. 2002. Production and biotransformation of 6-pentyl-α-pyrone by *Trichoderma harzianum* in two-phase culture systems. *Applied Microbiology and Biotechnology* 58:170–74
56. Hirpara DG, Gajera HP, Bhimani RD, Golakiya BA. 2016. The SRAP based molecular diversity related to antifungal and antioxidant bioactive constituents for biocontrol potentials of *Trichoderma* against *Sclerotium rolfsii* Scc. *Current Genetics* 62:619–41
57. Lee S, Yap M, Behringer G, Hung R, Bennett JW. 2016. Volatile organic compounds emitted by *Trichoderma* species mediate plant growth. *Fungal Biology and Biotechnology* 3:7
58. Daccò C, Nicola L, Temporiti MEE, Mannucci B, Corana F, et al. 2020. *Trichoderma*: evaluation of its degrading abilities for the bioremediation of hydrocarbon complex mixtures. *Applied Sciences* 10:3152
59. Dini I, Marra R, Cavallo P, Pironti A, Sepe I, et al. 2021. *Trichoderma* strains and metabolites selectively increase the production of volatile organic compounds (VOCs) in olive trees. *Metabolites* 11:213
60. Gajera HP, Hirpara DG, Savaliya DD, Golakiya BA. 2020. Extracellular metabolomics of *Trichoderma* biocontroller for antifungal action to restrain *Rhizoctonia solani* Kuhn in cotton. *Physiological and Molecular Plant Pathology* 112:101547
61. Pavirhra R, Lalitha S. 2020. Tetradecane producing biocontrol agent, *Trichoderma* spp. against *Fusarium oxysporum* in tomato (*Solanum lycopersicum* L.). *International Journal of Agricultural Technology* 16:1475–92
62. Zhan X, Khan RAA, Zhang J, Chen J, Yin Y, et al. 2023. Control of postharvest stem-end rot on mango by antifungal metabolites of *Trichoderma pinnatum* LS029-3. *Scientia Horticulturae* 310:111696
63. Shavkiev J, Kholmamatovich KH, Ismoilovna TB, Kizi ANS, Khodjakbarovich NM, et al. 2022. Some volatile metabolites produced by the antifungal-*Trichoderma asperellum* UZ-A4 micromycete. *International Journal of Phytopathology* 11:239–51
64. Filippovich SY, Bachurina GP. 2021. Nitric Oxide in Fungal Metabolism. *Applied Biochemistry and Microbiology* 57:694–705